iScience

Article

Attenuation processes in positive social emotion upregulation: Disentangling functional role of ventrolateral prefrontal cortex

Graphical abstract

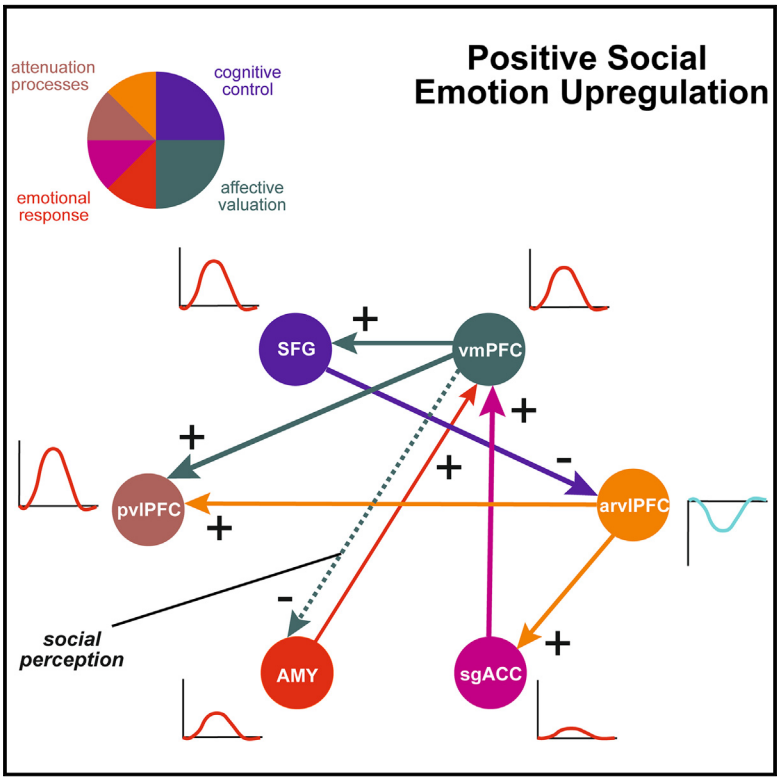

Highlights

- Healthy women performed upregulation of positive social emotions
- Distinct brain activity and connectivity patterns in vlPFC revealed
- Attenuation of arvlPFC activity under control influences of SFG modulated by vmPFC
- Individual perception of sociality mediates affective and social appraisals

Authors

Dmitriy D. Bezmaternykh, Mikhail Ye. Melnikov, Evgeny D. Petrovskiy, ..., Mark B. Shtark, Patrik Vuilleumier, Yury Koush

Correspondence

yurykoush@gmail.com

In brief

Neuroscience; Behavioral neuroscience

Bezmaternykh et al., 2025, iScience *28*, 111909
February 21, 2025
https://doi.org/10.1016/j.isci.2025.111909

CellPress

iScience

CellPress
OPEN ACCESS

Article

Attenuation processes in positive social emotion upregulation: Disentangling functional role of ventrolateral prefrontal cortex

Dmitriy D. Bezmaternykh,[1] Mikhail Ye. Melnikov,[1,2] Evgeny D. Petrovskiy,[3] Ksenia G. Mazhirina,[1] Andrey A. Savelov,[3] Mark B. Shtark,[1] Patrik Vuilleumier,[4,5] and Yury Koush[6,7,8,*]

[1]Institute of Molecular Biology and Biophysics, Federal Research Center of Fundamental and Translational Medicine, Novosibirsk, Russia
[2]Department of Biophysics, Biomedicine, and Neuroscience, Faculty of Biology and Biotechnology, Al-Farabi Kazakh National University, Almaty, Kazakhstan
[3]International Tomography Center SB RAS, Novosibirsk, Russia
[4]Department of Neuroscience, Medical School, University of Geneva, Geneva, Switzerland
[5]Swiss Center of Affective Sciences, University of Geneva, Campus Biotech, Geneva, Switzerland
[6]Vladimir Zelman Center for Neurobiology and Brain Rehabilitation, Skolkovo Institute of Technology, Moscow, Russia
[7]Department of Biomedical Engineering, Yale University, New Haven, CT, USA
[8]Lead contact
*Correspondence: yurykoush@gmail.com
https://doi.org/10.1016/j.isci.2025.111909

SUMMARY

Positive emotions determine individual well-being and sustainable social relationships. Here, we examined the neural processes mediating upregulation of positive social emotions using functional magnetic resonance imaging in healthy female volunteers. We identified brain regions engaged in upregulation of positive social emotions and applied a parametric empirical Bayes approach to isolate modulated network connectivity patterns and assess how these effects relate to individual measures of social perception. Our findings indicate that upregulation of positive social emotions shapes the functional interplay between affective valuation and cognitive control functions. We revealed a selective increase of bilateral posterior ventrolateral prefrontal cortex (vlPFC) activity and attenuation of activity in right anterior vlPFC under control influences from more superior prefrontal regions. We also found that individual perception of sociality modulates connectivity between affective and social networks. This study expands our understanding of neural circuits required to balance positive emotions in social situations and their rehabilitative potential.

INTRODUCTION

Positive emotions support psychological resilience, individual and societal well-being, and sustainable relationships.[1–4] Conversely, a lack of positive attitude to social events, known as social anhedonia, affects social functioning and may contribute to neuropsychiatric conditions, including schizophrenia, post-traumatic stress, and depressive disorders.[4–6] The recent COVID-19 pandemic and associated restrictions led to higher social anxiety[7] and radically altered interpersonal interactions that typically support social-emotional well-being.[8,9]

Previous research on emotion regulation suggests that decreasing response to negative emotions requires inhibiting prepotent appraisal of a stimulus in favor of an alternative reappraisal, and that these processes are associated with activation of ventrolateral prefrontal cortex (vlPFC),[10–13] which is thought to play an inhibitory role across several other tasks.[14–16] The prefrontal control system may also suppress overactive pleasure, a process that might lead to depression in people with mood disorders due to inappropriate activation. Accordingly, depressed patients who demonstrate less downregulation of positive emotions show quicker and better recovery from anhedonia in response to antidepressant treatment, associated with lower activity in rvlPFC, relative to patients with more persistent anhedonia who may exert stronger inhibition of positivity.[17] On the other hand, transcranial magnetic stimulation (TMS) studies reported that suppression of rvlPFC activity can lead to more negative appraisal, whereas its activation can lead to less negative appraisal during regulation of negative emotions.[18] Likewise, activation of rvlPFC is associated with more positive social evaluation,[18] relief of social pain, and increased reward.[19] However, the engagement of vlPFC in successful generation and regulation of negative emotions is also dependent on positive mediators, including nucleus accumbens/ventral striatum and subgenual anterior cingulate cortex (sgACC) that is associated with greater reappraisal success, and negative mediators such as amygdala, associated with lower reappraisal success.[12] In sum, the exact role of rvlPFC in emotion regulation remains unresolved. It is unclear whether this region primarily mediates regulation processes by suppressing negative affect, enhancing

positive affect, or dampening instead both positive and negative emotions. More generally, the involvement of vlPFC (in tandem with homologous regions in left hemisphere) during reappraisal of negative emotions might be related to more demanding control goals compared to upregulation of positive emotions, as well as to differences between approach and avoidance processes modulated by regulation strategies.[10]

Unlike emotion self-regulation where the regulator and the target are the same person, social regulation of emotions refers to process where an individual attempts to regulate the emotional response of another individual(s).[20] Nonetheless, both social regulation and self-regulation of emotions in social situations may recruit similar brain structures,[20–23] including interactions between higher-order regions for cognitive control and affective networks.[20] It is well-established that a key neural mechanism of emotion regulation is the top-down influence from prefrontal cortices onto emotion generating system, primarily onto amygdala.[24,25] Amygdala plays a central role in conscious and unconscious emotion processing and essentially acts to extract the meaning of social signals.[26–28] In addition, sgACC transfers information from limbic to cognitive control system,[29–31] supports social processing,[32,33] and promotes positive social emotion regulation.[21,31] Other crucial brain regions for the regulation of positive social emotions include ventromedial prefrontal cortex (vmPFC),[21] a key part of affective, social, and reward processing systems[34–39]; whereas dorsomedial (dmPFC) and lateral prefrontal cortices are implicated in more general cognitive control systems,[10,37] and engaged in positive social emotion upregulation along with superior frontal gyrus (SFG) adjacent to dmPFC.[21,31]

However, the regulation of positive and positive social emotions remains much less studied as compared to negative emotion regulation,[10,40,41] which limits our mechanistic understanding of emotion regulation processes. Moreover, growing evidence suggests that different emotion regulation goals and different levels of stimulus valence may involve both common and distinct brain structures.[22,40] Recent research also indicates that cognitive up- and downregulation of emotions involves activation of partly similar brain regions including, among others, bilateral vlPFC and dorsomedial PFC (dmPFC).[21,40–42] Activation of vlPFC was primarily observed during reappraisal of negative emotions,[11–13] and most recently, during reappraisal regardless of valence,[40,43] also known as anterior inferior frontal gyrus involved in inhibitory control.[44,45] However, it remains unclear whether vlPFC modulates positive social emotion regulation network.

To address these open questions, we used functional MRI (fMRI) experiments requiring active self-engagement in positive social situations and upregulation. By focusing on vlPFC as a key region, we studied activation in positive social situations compared to viewing neutral social situations and applied dynamic causal modeling (DCM) to probe for the interplay between this region and other brain areas implicated in emotion regulation. Distinct alternative models were examined to unveil how vlPFC mediates affective and control processes during positive social upregulation. To enable robust behavioral and fMRI analyses of individual data, we acquired two fMRI runs per participant and introduced rest periods between regulatory trials. Unlike structural and resting state functional connectivity, our effective connectivity analysis allowed us to investigate causal influences between interconnected brain areas together with their modulation by contextual factors and stimuli, through group-level DCM analysis and parametric empirical Bayes (PEB).[46,47] We hypothesized that vlPFC would be more active during positive social upregulation if it directly acts to increase positive affect. Alternatively, vlPFC should be either less active or show no change if it mediates a more general suppression of affect regardless of valence, as suggested by previous research on reappraisal of negative emotions.[12] In addition, positive emotion upregulation in social situations should recruit other regions implicated in affective processing, social cognition, and cognitive control, which might interact with vlPFC through either attenuating or enhancing modulatory influences according to the exact role of this region in affective and control processes. We therefore hypothesized selective connectivity changes in DCM results. Thus, we expected that vlPFC might exert direct influences onto limbic and affect valuation regions, receive modulatory inputs from other cognitive control regions, and show context-dependent modulations of these connections during the positive social emotion upregulation task. Given that vlPFC (de)activation was not explicitly disambiguated during upregulation of positive emotions in the past literature, we had no hypothesis about the sign of these interactions. In addition, we hypothesized that connectivity strength between vlPFC and other brain regions could be predicted by individual perception of sociality in emotion eliciting situations. Since positive social upregulation is associated with prosocial behavior,[18,19,48–50] understanding neural processes controlling positive social emotion upregulation may help better assessing and preventing dysregulations that can lead social exclusion on mood and well-being.

RESULTS

We investigated attenuation processes in positive social emotion upregulation and the role of rvlPFC in this regulation in a group of healthy female volunteers using two whole-brain fMRI experiments. We modeled PEB variations of endogenous connectivity and contextual modulations of positive social emotion regulation network with individual sociality scores as covariates, and specifically investigated the functional interplay of activated bilateral posterior ventrolateral prefrontal cortex (pvlPFC) and deactivated right anterior vlPFC (arvlPFC) with positive social emotion regulation network and the influence of individual social perception.

Behavioral ratings and questionnaire scores

For the first experiment, behavioral results were reported elsewhere[21] but did not distinguish valence from (non-)sociality ratings. For the second experiment (Figure 1), participants reported good adherence to the experimental protocol (ability to focus: 3.7 ± 1.9) and moderate vividness of imagery (2.1 ± 2.7). Participants did not increase positive affect after compared to before the experiment (Figure 2A, Table S1; PANAS-P, before: 56.4 ± 12.4, after: 56.7 ± 13.4, paired one-tailed t-test, $t_{19} = 0.13$, $p = 0.89$), but showed a trend decrease in negative affect (PANAS-N, before: 20.5 ± 3.1, after: 19.4 ± 2.3, paired one-tailed t-test, $t_{19} = 1.72$, $p = 0.051$). This lack of increase in positive affect and trend reduction of negative affect is consistent with past

research using similar duration and intensity of positive social stimuli.[21] Participants consistently rated positive social pictures with higher valence, arousal, and sociality scores, confirming that positive social situations were perceived as more pleasant and socially engaging interactions than the neutral social situations in our dataset (Figure 2A; valence: positive, 7.33 ± 0.53; neutral, 5.49 ± 0.39; paired t-test, $t_{19} = 19.55$, $p < 0.001$; arousal: positive, 6.46 ± 1.03; neutral, 4.93 ± 1.15, paired t-test, $t_{19} = 17.69$, $p < 0.001$; sociality: positive, 6.31 ± 0.98; neutral, 4.86 ± 1.00; paired t-test, $t_{19} = 9.80$, $p < 0.001$). We also found significant correlations between scores of positive and neutral pictures (Figure 2B; valence, r = 0.62, $p = 0.004$; arousal, r = 0.94, $p < 0.001$; sociality, r = 0.78, $p < 0.001$). There were no correlations between sociality and valence (positive, r = 0.21, $p = 0.37$; neutral, r = 0.28, $p = 0.23$) or arousal (positive, r = 0.33, $p = 0.16$; neutral, r = 0.35, $p = 0.13$) scores. In line with prior work, we did not find associations between avoidance attachment style scores and valence ratings of social situations.[51] Interestingly, we observed a significant positive correlation between avoidance attachment style (ECR-AVS) scores and sociality scores of social neutral images (Figure 2C, r = 0.71, adjusted $p = 0.037$, FDR correction across all questionnaires and behavioral ratings applied, $n = 300$, $q < 0.05$). Higher avoidant attachment scores were associated with higher individual sociality ratings of neutral social situations (not positive), suggesting that participants who tend to feel uncomfortable with intimacy treated neutral social scenes as more socially engaging relative to non-avoidant participants.

Brain activity associated with positive social emotion upregulation

For the first experiment, the main effect of upregulation (upregulation vs. viewing) revealed activations in SFG, and the main effect of positive social stimuli (positive social vs. neutral nonsocial) revealed, among other brain areas, activations in dmPFC, vmPFC, sgACC, and bilateral amygdala. The specific effect of upregulating positive social emotions compared to passive viewing of positive social pictures was associated with increased activity of SFG and dmPFC (Table S2, details reported elsewhere[21]). This experiment did not reveal arvlPFC (de)activation when comparing other upregulation and passive viewing conditions.

For the second experiment, blocks with upregulation of positive social emotion (in comparison to passive viewing of neutral social pictures) activated a widespread network including bilateral SFG, dmPFC, bilateral amygdala, vmPFC, left anterior insula, inferior frontal gyrus (IFG/pvlPFC), thalamus/caudate, hippocampus, putamen, superior temporal sulcus, and superior parietal lobule (Figure 3A, Table S2, upregulate positive social > view neutral social). Conversely, this comparison was also associated with significant decrease in arvlPFC, as well as inferior parietal lobule, superior and middle temporal gyri, and medial regions overlapping with default mode network (Figure 3A, Table S2, view neutral social > upregulate positive social). The upregulation of positive social emotion in comparison to fixation also shared similar effects than those in the first experiment, with activation in dmPFC, vmPFC, sgACC, pvlPFC, and left temporoparietal junction (TPJ), among other areas (Figure 3B, Table S2, upregulate positive social > fixation). These results therefore reject the hypothesis that arvlPFC would be activated stronger during positive social upregulation as compared to neutral social situations. Instead, bilateral pvlPFC was activated and arvlPFC was deactivated. Consistently with previous findings on selective processing of social stimuli,[27] we did not find any functional lateralization of amygdala activity (comparing individual contrast images with their flipped counterparts) but observed a specialization of the superficial part of amygdala

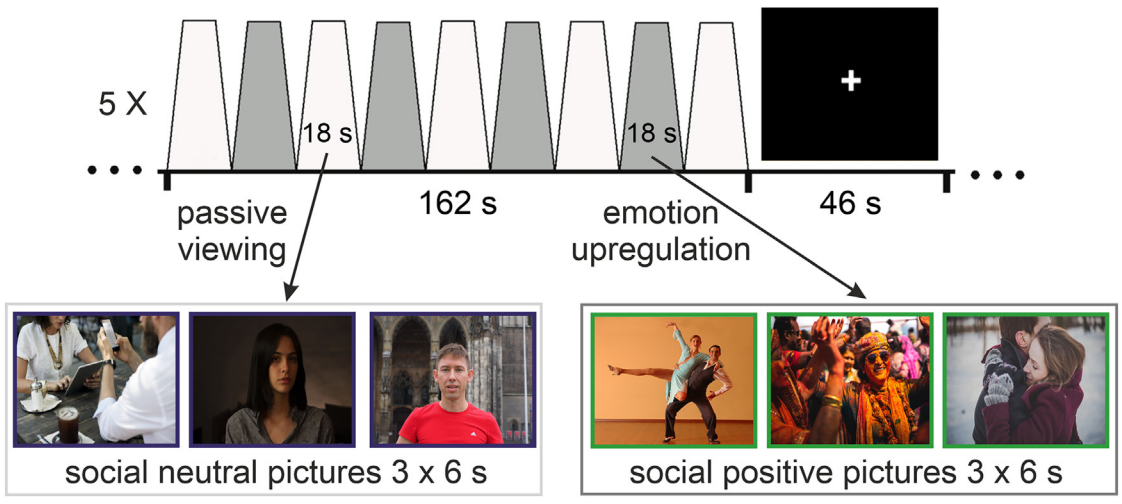

Figure 1. Design of a functional run in experiment 2

During two functional runs, alternating blocks of neutral and positive social pictures were presented via MR-compatible monitor (17.6 min run duration). Each run included five trials that comprised four upregulation blocks interleaved with five passive viewing blocks of 18 s each, followed by a 46 s fixation period (3 social pictures per block with 6 s display duration). Participants were instructed to passively look at neutral social situations (blue frame; passive viewing) or imagine experiencing positive social situations from a first-person perspective and feel positive about it (green frame; emotion upregulation). For illustrative purposes, we used social pictures found via Google search engine under the Creative Common Zero license.

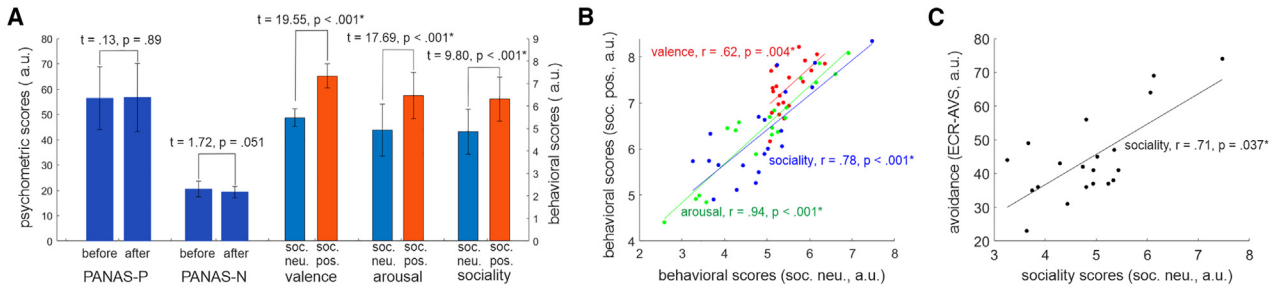

Figure 2. Psychometric scores and correlations between behavioral characteristics

(A) Emotion regulation (during experiment 2) did not increase positive mood but showed a trend-level decrease in negative mood. Positive social pictures were rated significantly higher than neutral social pictures in valence, arousal, and sociality. For average values, we reported the mean and standard deviation (SD). * indicate statistical significance ($p < 0.05$).

(B) Higher individual scores of positive social images were associated with higher scores of social neutral images, indicating high consistency of social scene ratings within a participant. * denote significant Pearson correlations ($p < 0.05$).

(C) Higher attachment avoidance scores were associated with higher sociality scores of neutral social pictures, suggesting that participants who seek independence and tend to experience discomfort from intimacy perceived neutral social scenes as more convenient for social interaction (while this relation was not significant for positive social scenes, r = 0.58, $p = 0.15$). * Survived FDR correction for multiple comparisons (across all questionnaires and behavioral ratings, $n = 300$, $q < 0.05$).

activity during upregulation of positive social emotions (Table S3). In addition to superficial part of amygdala, elicited activation in basolateral complex in upregulation condition related to fixation could be associated with social perception.[52]

Regression analyses revealed that individual sociality scores of neutral social pictures correlated negatively with upregulation vs. neutral viewing activity in bilateral amygdala (Figure 3C, $r = -0.69$, adjusted $p = 0.005$; FDR-corrected for multiple comparisons across ROIs, $n = 6$, $q < 0.05$). The cognitive reappraisal (ERQ-R) scores were also negatively correlated with upregulation activity vs. neutral viewing in bilateral amygdala and sgACC (Figure 3D, amygdala: $r = -0.61$, adjusted $p = 0.014$, sgACC: $r = -0.63$, adjusted $p = 0.014$; FDR-corrected for multiple comparisons across ROIs, $n = 6$, $q < 0.05$). Despite the BDI scores being relatively low (mean ± SD, 3.9 ± 3.3), they correlated negatively with upregulation activity in pvlPFC (Figure S1, $r = -0.58$, adjusted $p = 0.043$, FDR-corrected for multiple comparisons across ROIs, $n = 6$, $q < 0.05$).

Effective connectivity in positive social emotion upregulation

To further investigate regulation processes modulated by rvlPFC and identify network parameters associated with subjective sociality ratings, we performed an effective connectivity analysis using hierarchical PEB framework. We specifically focused on disentangling the functional roles of activated pvlPFC and deactivated arvlPFC during positive social emotion upregulation (Table S2), given the known reappraisal role of bilateral pvlPFC regardless of valence,[40,43] its engagement in reappraisal of negative emotions,[10–13] regulation of social emotions,[19] and inhibitory control.[44,45] Thus, we defined key network nodes including bilateral pvlPFC, arvlPFC, vmPFC, sgACC, bilateral SFG that included dmPFC, and bilateral amygdala. Positive and negative DCM PEB connectivity strengths indicate excitatory and inhibitory influences, respectively. Negative self-connectivity of nodes indicates decreased self-inhibition (i.e., disinhibition), expressed in terms of the log-scaled self-inhibitory prior $-0.5*\exp(A_{i,i})$.

When considering PEB variations of endogenous connectivity, we found a highly interconnected network (Figure 4A, model with sociality covariate of positive pictures). The strongest excitatory influence was exerted from sgACC onto pvlPFC and from pvlPFC onto SFG. Interestingly, pvlPFC had positive outgoing endogenous connections with all other nodes of the model except arvlPFC. Conversely, arvlPFC received a single selective attenuating influence from pvlPFC and exerted an excitatory influence onto pvlPFC and SFG. We also examined the PEB variations of endogenous connectivity with sociality covariate of neutral pictures, which revealed a network architecture generally similar to model variations with the sociality covariate of positive pictures (Figure S2A). They differed in additional inhibitory connection of vmPFC onto arvlPFC and lack of sgACC onto AMY endogenous positive connectivity. An inhibitory influence of vmPFC onto arvlPFC suggests that in presence of deactivation of arvlPFC, more active regulatory processes were required to evaluate neutral social situations, assign affective values to these situations, and assess their personal self-relevance.

We then determined contextual PEB variations of this network related to positive social upregulation demands. The effect of emotion upregulation task was such that AMY and sgACC positively modulated affective valuation in vmPFC, which in turn positively modulated pvlPFC and SFG (Figure 4B). Furthermore, SFG strongly attenuated arvlPFC, which in turn positively modulated sgACC and pvlPFC. Thus, we confirmed our hypothesis that rvlPFC areas exerted direct influences onto limbic and affective systems and were contextually modulated by emotion upregulation demands via attenuating connectivity from cognitive control system (i.e., SFG). However, we also observed distinct interactions between pvlPFC and arvlPFC with the rest of the network. When considering PEB variations of contextual connectivity models with sociality covariate of neutral pictures, emotion upregulation task modulated not only SFG onto arvlPFC inhibitory influence, but also outgoing arvlPFC onto SFG connectivity (Figure S2B).

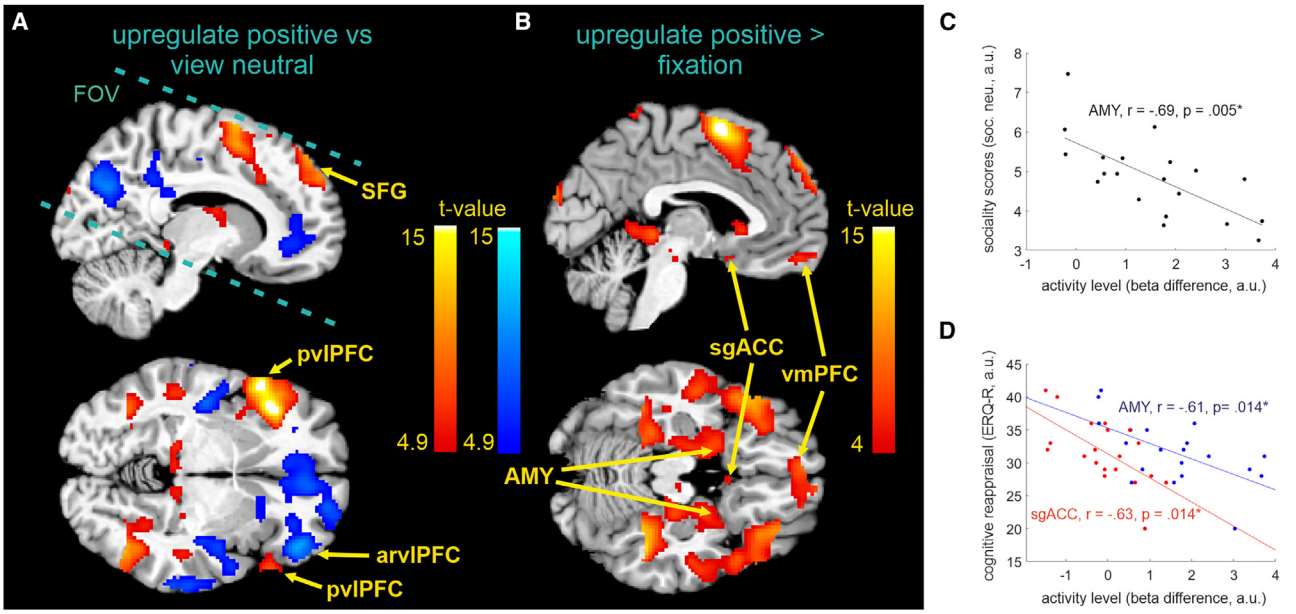

Figure 3. Brain activations and their associations with sociality and cognitive reappraisal scores in experiment 2

(A) Upregulation of positive social emotions compared to passive viewing of neutral social situations was associated with increased (red scale) activity in SFG, vmPFC, pvlPFC and bilateral amygdala, as well as decreased (blue scale) activity in arvlPFC and DMN (FWE, $p < 0.05$). For illustration purposes, activation maps were threshold at FWE $p < 0.05$.

(B) In upregulation contrasted to fixation we additionally observed significant activations in sgACC (FWE, $p < 0.05$). For illustration purposes, activation maps were threshold at $p < 0.005$ unc.

(C) Higher sociality scores of neutral social pictures predicted lower and negative changes in bilateral amygdala activity during positive social emotion upregulation, indicating that individuals with stronger ability to socialize in neutral social content exhibited lower emotional responses.

(D) Higher cognitive reappraisal scores predicted lower and negative activity changes in bilateral amygdala and sgACC during upregulation, indicating that individuals with higher reappraisal preferences showed lower emotional responses.

(C and D) * survived FDR correction for multiple comparisons (across ROIs, $n = 6$, $q < 0.05$).

We also examined how these functional networks were modulated by the individual social perception of positive scenes. Although individual ratings of positive social and neutral social pictures were correlated, we estimated two separate PEB variations of endogenous connectivity and their contextual modulations using sociality ratings of neutral and positive social pictures as distinct covariates, respectively. When considering PEB variations of endogenous connectivity, sociality ratings of positive pictures were positively associated with endogenous connectivity from SFG onto vmPFC, vmPFC onto pvlPFC, and from AMY onto pvlPFC and arvlPFC (Figure 4C; for neutral pictures, see Figure S2). In parallel, they were negatively associated with the endogenous connectivity from sgACC onto AMY and pvlPFC, pvlPFC onto vmPFC, and from SFG onto pvlPFC. Sociality ratings of positive and neutral pictures also modulated disinhibition self-connectivity of AMY and arvlPFC nodes. These data confirm our hypothesis that connectivity strength between arvlPFC and AMY engaged in socio-affective processes could be predicted by individual traits making sociality effects complementary to the effects of regulation. When considering contextual PEB variations related to upregulation demands, we found significant negative association between sociality ratings of positive pictures and contextual connectivity from vmPFC onto AMY during emotion upregulation (Figure 4B, dashed line). In comparison to positive pictures, models of endogenous connectivity with sociality covariate of neutral pictures were characterized with additional positive associations between sociality scores and connectivity from SFG onto sgACC, AMY onto vmPFC, and negative associations between sociality scores and connectivity from sgACC onto vmPFC (Figure S2C). Distinctively from sociality perception of positive scenes, this network had no associations for connectivity from SFG and vmPFC onto pvlPFC, and from sgACC onto AMY. The negative association between contextual modulation of connectivity from vmPFC onto AMY and sociality ratings was not found for neutral social pictures.

Finally, for fully connected DCM models, we post-hoc illustrated a positive association between individual sociality ratings of positive pictures and arvlPFC disinhibition self-connectivity (Figure 4D, one-tailed Pearson r = 0.49, $p = 0.013$ unc.), and a positive association with endogenous connectivity strength from AMY onto arvlPFC (Figure 4E, one-tailed Pearson r = 0.38, $p = 0.047$ unc.). We also plotted the only significantly negative contextual modulation by social perception, namely connectivity from vmPFC onto AMY (Figure 4F, one-tailed Pearson r = −0.53, $p = 0.008$ unc.).

DISCUSSION

Regulation of positive and positive social emotions remains much less studied as compared to negative emotion regulation.

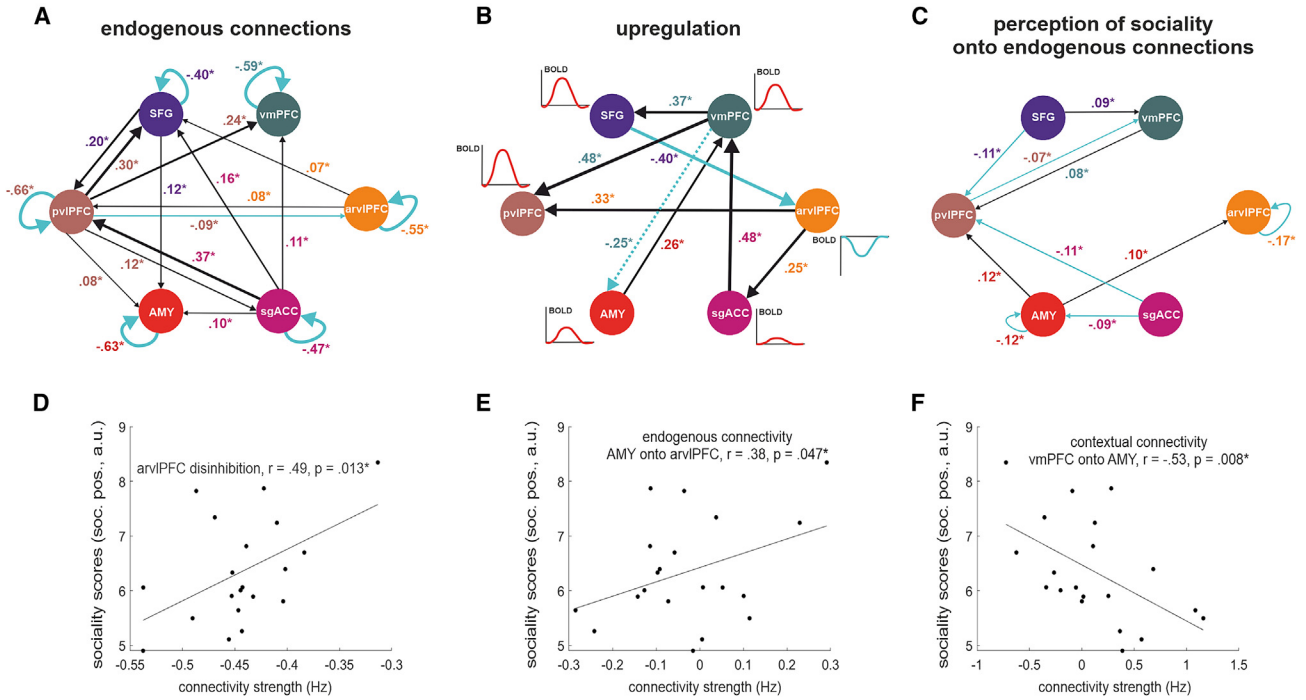

Figure 4. Effective connectivity underlying positive social emotion upregulation

To evaluate directional connections between nodes, we varied PEB models of endogenous and contextual modulation connectivity with sociality scores of positive social pictures as covariates. The numbers and thickness of the arrows indicate BMA values (cyan arrows for negative and black arrows for positive connectivity strengths).

(A) The group average endogenous connectivity revealed a highly interconnected network. The pvlPFC showed positive connections with all the other network nodes except arvlPFC, and arvlPFC received a single attenuating influence from pvlPFC and exerted an excitatory influence onto pvlPFC and SFG.

(B) The emotion upregulation task positively modulated connectivity from AMY and sgACC onto vmPFC, which positively modulated pvlPFC and SFG. Moreover, SFG attenuated arvlPFC, which in turn positively modulated sgACC and pvlPFC, indicating highly selective changes in the interplay between control processes mediated by pvlPFC and arvlPFC. Illustrative brain activity waveforms were scaled proportionally to the contrast-to-noise-ratio of the corresponding nodes (average CNR estimated for upregulate positive vs. view neutral contrast; 0.19 for bilateral AMY, 0.45 for bilateral pvlPFC, 0.36 for bilateral SFG and dmPFC, −0.24 for arvlPFC, and 0.31 for vmPFC). Dashed line denotes significant negative association between sociality ratings of positive pictures and contextual connectivity from vmPFC onto AMY during emotion upregulation, illustrated on this panel for simplicity.

(C and D) Higher sociality scores of positive social pictures were associated with significantly increased disinhibition of arvlPFC and AMY, indicating increased sensitivity of these nodes to social content. In addition, sociality scores were associated with several endogenous connectivity strengths, including modulation of connectivity between pvlPFC and arvlPFC and the rest of the network, indicating that socio-affective processes could be predicted by individual traits. We showcased that sociality scores of positive pictures correlated positively with (D) magnitude of disinhibition of arvlPFC,

(E) connectivity strength from AMY onto arvlPFC, and negatively with (F) contextual connectivity from vmPFC onto AMY during positive social upregulation.

(A–C) * denote parameters with posterior probability (Pp) > 0.95 (strong evidence). (D–F) * denote significant post-hoc one-tailed Pearson correlations ($p < 0.05$ unc.).

Despite suggested similarity between negative and positive emotion regulation processes, e.g., on generic reappraisal role of activated bilateral pvlPFC,[40,43] there is growing evidence that different emotion regulation goals and emotional valence may involve distinct brain structures.[22,40] The present study provides new insights into the neural mechanisms underlying positive social emotion upregulation from a first-person perspective and the role of rvlPFC in this regulation in a group of healthy female volunteers using whole-brain fMRI.

Brain (de)activation related to positive social emotion upregulation

Upregulation of positive emotions in positive social situations as compared to viewing neutral social scenes confirmed an engagement of several brain regions typically implicated in cognitive reappraisal,[10,12,40] social processing,[20] and positive social emotion upregulation.[10,21,31] These involved limbic system (e.g., AMY, sgACC), higher-order prefrontal regions implicated in executive control and social cognition (e.g., SFG, dmPFC), and affect generation (e.g., vmPFC). As expected in both experiments, upregulation of positive social emotions was associated with significant activations of dmPFC and adjacent bilateral SFG regions implicated in cognitive control of emotions and social processing. Expectedly, SFG, dmPFC, vmPFC, TPJ, sgACC and bilateral amygdala were more active during upregulation of positive social emotions as compared to fixation baseline. Higher cognitive reappraisal scores predicted lower and negative activity changes in bilateral amygdala and sgACC during upregulation, suggesting that participants with larger emotion reappraisal capability also show lower recruitment of

emotion generation regions during positive social emotion upregulation.[21,31]

We also identified activation in bilateral pvlPFC, in line with prior studies on reappraisal of positive and negative emotions[40,43] and inhibitory control.[44,45] Interestingly, participants who scored lower on BDI showed greater bilateral pvlPFC activation, which is consistent with patients in depression compared to healthy controls during reappraisal of negative emotions.[13]

Identified deactivation of arvlPFC suggests distinct functional rvlPFC subdivisions and more general role in attenuating affect as reflected by increased recruitment for negative downregulation and additionally reduced recruitment for positive social upregulation. Functional segregation of rvlPFC was recently suggested in meta-analytic study,[43] where arvlPFC and pvlPFC were assigned to different co-activation groups implicated in response inhibition or executive control and appraisal or language processing during emotion regulation, respectively. Although it was suggested that these two networks support mainly the regulatory processes specific to reappraisal of negative emotions, perhaps due to the permanent literature shift toward negative emotion regulation.[10,40,41]

Implications of arvlPFC attenuation for mediation of affective appraisal

Self-referential positive social emotion upregulation revealed strong interconnections between prefrontal and limbic systems, which agrees with previous studies on positive social emotion regulation[21,31] and reappraisal of negative emotions.[10,12] Critically, contextual modulation of endogenous connectivity by emotion upregulation highlighted the key functional interplay of arvlPFC with affective valuation, cognitive control, and social emotion regulation network. This was evidenced by strongly attenuated contextual connectivity from SFG onto arvlPFC and positively modulated contextual connectivity from arvlPFC onto pvlPFC and sgACC. While functional role of SFG (dmPFC and adjacent SFG) is generally thought to mediate cognitive control during social emotional appraisal and introspection,[53,54] to evaluate social information,[55,56] to situate oneself in social contexts,[55,57] and to maintain a goal-relevant regulation strategy,[57] it also appears to be crucially engaged during positive social emotion upregulation.[21] Notably, we revealed direct interactions between SFG and pvlPFC but contextual modulation form SFG onto arvlPFC. Since rvlPFC is positively engaged in reappraisal of negative emotions and response inhibition,[14,44] deactivation of arvlPFC in positive upregulation of emotions in positive social situations in comparison to passive viewing of neutral social situations and its selective connectivity pattern with pvlPFC and SFG could be explained by distinctive roles of rvlPFC subdivisions in effect attenuation processes.

Excitatory influence of arvlPFC onto sgACC suggests its mediatory role in gatekeeping processes between limbic and prefrontal cortices in social cognition[32,33,35] and positive social emotion upregulation.[21,31] Moreover, higher cognitive reappraisal scores predicted lower activity changes in bilateral amygdala and sgACC, indicating that individuals with stronger preference for reappraisal as an emotion regulation strategy exhibit lower positive emotional response and weaker connectivity changes between limbic and prefrontal cortices.[31] This is well in line with findings on negative stimuli[58,59] and downregulation of negative emotions,[60,61] suggesting a coupling between preference to reappraise and amygdala responsivity irrespective of valence.

Observed contextual modulation during positive social emotion upregulation is largely consistent with prefrontal-subcortical interactions modulated by reappraisal success during negative emotion upregulation.[62] Specifically, authors observed positive correlation of negative emotion upregulation success with coupling of IFG (like pvlPFC) and amygdala, dmPFC and sgACC and amygdala, vmPFC and IFG, and negative correlation of upregulation success with coupling between IFG and dmPFC. Interestingly, they also found reversed correlation pattern between vmPFC and IFG during negative emotion downregulation (via distancing from negative situations). Therefore, for emotion upregulation regardless of valence, vmPFC was found positively associated with pvlPFC, while reappraisal of negative emotions reversed this dependency, confirming a key role of pvlPFC in regulation of positive social emotions as in regulation of negative emotions[62] and in regulation of social emotions on a regulator side.[20]

Notably, we did not reveal direct interactions between vmPFC and arvlPFC regions but between vmPFC and pvlPFC, as well as contextual connectivity from vmPFC onto pvlPFC. Widespread endogenous connectivity pattern of pvlPFC and contextual connectivity from vmPFC and arvlPFC onto pvlPFC could reflect its mediatory role in positive social emotion regulation processes. This finding is consistent with positive effective connectivity between vmPFC and left IFG (i.e., pvlPFC) in upregulation of aversive stimuli.[62] Additionally, positive social upregulation task modulated affective appraisal through the excitatory influence of sgACC and AMY onto vmPFC, which was further translated to SFG and pvlPFC. This is consistent with the known mediatory role of vmPFC in prefrontal-subcortical connectivity.[12,21,63,64] The role of vmPFC is also central in regulation of social emotions, connecting social engagement with affective and reward systems,[34,35,38] as it computes mainly affective valuations and is modulated by both sociality and valence dimensions,[65,66] assigning and updating the subjective value of stimuli.[37,39]

Implications of arvlPFC attenuation and sociality perception for mediation of social appraisal

Bilateral amygdala plays a prominent role in evaluating social cues and facial expressions.[23,26,28] Here, lower individual sociality scores of neutral social pictures predicted higher activation in bilateral amygdala during emotion upregulation. This suggests that participants with larger emotion upregulation capability and greater recruitment of emotion generation regions might perceive neutral social situations as less suitable for social interaction, which fits with the notion that amygdala activity is modulated by sociality dimension.[22,65,67]

Our endogenous connectivity models revealed significant associations between connectivity strength and perceived sociality of positive and neutral social pictures. Specifically, higher individual sociality scores were associated with reduction in self-inhibition inputs for bilateral AMY and arvlPFC, and with higher positive connectivity from AMY onto arvlPFC and pvlPFC. This suggests increased sensitivity of these regions to activity in the rest of the network mediated by the perception of sociality in positive social situations.[68]

For sociality covariates of neutral pictures, we identified negative associations for connectivity from SFG onto arvlPFC as compared to connectivity from SFG onto pvlPFC for positive pictures. This indicates specific top-down regulatory processes in social situations reflected in inverse coupling between putative attenuation processes mediated by arvlPFC and/or pvlPFC and individual perception of sociality of social situations. The coupling between sociality perception and arvlPFC disinhibition complements prior findings that increases or decreases of rvlPFC activity by TMS distinctively modulate emotions and prosocial behavior,[18] while TMS-induced activation of rvlPFC improves positive memory regarding social feedback.[19]

Individual perception of sociality mediated connectivity from SFG onto pvlPFC and vmPFC and reciprocal connectivity between pvlPFC and vmPFC in positive social situations as well as connectivity from SFG onto arvlPFC, vmPFC and sgACC and from pvlPFC onto vmPFC in neutral social situations, which indicates that attenuation processes are integrated in both the affective valuation of social situations and cognitive control processes. Accordingly, a mediatory role of vmPFC and rvlPFC was also suggested by TMS-induced activation of rvlPFC which demonstrated attenuated activity in amygdala and insula but enhanced coupling of prefrontal-subcortical areas via vmPFC during the reappraisal of negative social exclusion.[63]

Conclusions

Contrary to common observations of rvlPFC activation during reappraisal of negative emotions, we identified an increase of bilateral pvlPFC activity and specific decrease of arvlPFC activity during the upregulation of positive social emotions, as compared to passive viewing of neutral social situations. Our findings suggest that arvlPFC function might be attenuated during the effortful self-engaged positive social emotion upregulation, and that perception of sociality of positive and neutral social situations also modulates these processes. We show evidence that upregulation of positive social emotions involves attenuation processes that modulate the network interplay between several brain regions implicated in affective and social appraisal, and cognitive control processes. This knowledge advances our understanding of neural circuits related to balancing upregulation of positive emotions in social situations and explores the rehabilitative potential of modulating different parts of this network.

Limitations of the study

There were several limitations to the current study design. The all-female sample limits our ability to generalize the results and examine potential sex differences. However, female participants may show stronger emotional responses and larger regulation effects in both PFC and subcortical areas, as compared to males, particularly for positive emotions and reappraisal.[69,70] This gender selection served to optimize the sensitivity of our measures. In addition, we focused on a realistic scenario of therapeutic relevance engaging oneself in positive social emotions.[21,31,71,72] However, our data were collected across two separate experiments. Because the first experiment allows contrasting upregulation and passive viewing of positive social situations, the second experiment included only the upregulation of positive social pictures versus passive viewing of neutral social pictures,[12] allowing to most effectively capture upregulation effects for social stimuli.[73] Nevertheless, the current design does not allow for determining whether the observed effects are due to emotional valence, context type, or their interaction, which has been done elsewhere.[22,40] Our findings motivate future research revisiting balanced positive, neutral, and negative social study designs to shed more light on specificity of emotion regulation processes.

RESOURCE AVAILABILITY

Lead contact

Further information and requests for resources should be directed to the lead contact, Yury Koush, (yurykoush@gmail.com).

Materials availability

This study did not generate plasmids, mouse lines, or unique reagents.

Data and code availability

- Code: the code generated during conventional data analyses is based on SPM12 and MATLAB functions and is available from the lead contact upon request.
- Data: group-level fMRI and DCM results reported in the present study are available from OSF (OSF: https://osf.io/8tvec/). The single subjects' raw MRI data reported in this study cannot be deposited in a public repository due to restrictions imposed by the local ethics committee.
- Additional information: all data needed to evaluate the conclusions in this paper are available within the paper and the Supplemental Information. Any additional information required to reanalyze the data reported in this paper is available from the lead contact upon request.

ACKNOWLEDGMENTS

The study was supported by the Russian Science Foundation (project no. 21-15-00209).

AUTHOR CONTRIBUTIONS

The authors confirm contribution to the study as follows: conceptualization: M.Y.M. and Y.K.; investigation and methodology: D.D.B., M.Y.M., E.D.P., K.G.M., A.A.S., M.B.S., and Y.K.; data analyses: D.D.B. and Y.K.; supervision: Y.K.; writing and edits: D.D.B., M.Y.M., P.V., and Y.K. All authors approved the final version of the manuscript.

DECLARATION OF INTERESTS

The authors declare no competing interests.

STAR★METHODS

Detailed methods are provided in the online version of this paper and include the following:

- KEY RESOURCES TABLE
- EXPERIMENTAL MODEL AND STUDY PARTICIPANT DETAILS
  - Participants
  - Informed consent and ethics approval
- METHOD DETAILS
  - Stimuli
  - Experimental paradigm
  - MRI data acquisition
  - fMRI data preprocessing
- QUANTIFICATION AND STATISTICAL ANALYSIS
  - GLM analysis
  - Dynamic causal modeling
  - Analyses of the behavioral and psychometric data

SUPPLEMENTAL INFORMATION

Supplemental information can be found online at https://doi.org/10.1016/j.isci.2025.111909.

Received: February 29, 2024
Revised: September 27, 2024
Accepted: January 23, 2025
Published: January 27, 2025

REFERENCES

1. Diener, E., Napa Scollon, C., and Lucas, R.E. (2009). The Evolving Concept of Subjective Well-Being: The Multifaceted Nature of Happiness. In Assessing Well-Being: The Collected Works of Ed Diener, E. Diener, ed. (Springer Netherlands), pp. 67–100. https://doi.org/10.1007/978-90-481-2354-4_4.
2. Fredrickson, B.L. (2001). The role of positive emotions in positive psychology. The broaden-and-build theory of positive emotions. Am. Psychol. *56*, 218–226. https://doi.org/10.1037//0003-066x.56.3.218.
3. Kok, B.E., Coffey, K.A., Cohn, M.A., Catalino, L.I., Vacharkulksemsuk, T., Algoe, S.B., Brantley, M., and Fredrickson, B.L. (2013). How positive emotions build physical health: perceived positive social connections account for the upward spiral between positive emotions and vagal tone. Psychol. Sci. *24*, 1123–1132. https://doi.org/10.1177/0956797612470827.
4. Mauss, I.B., Shallcross, A.J., Troy, A.S., John, O.P., Ferrer, E., Wilhelm, F.H., and Gross, J.J. (2011). Don't hide your happiness! Positive emotion dissociation, social connectedness, and psychological functioning. J. Pers. Soc. Psychol. *100*, 738–748. https://doi.org/10.1037/a0022410.
5. Pelizza, L., and Ferrari, A. (2009). Anhedonia in schizophrenia and major depression: state or trait? Ann. Gen. Psychiatry *8*, 22. https://doi.org/10.1186/1744-859X-8-22.
6. Barkus, E., and Badcock, J.C. (2019). A Transdiagnostic Perspective on Social Anhedonia. Front. Psychiatry *10*, 216. https://doi.org/10.3389/fpsyt.2019.00216.
7. Kindred, R., and Bates, G.W. (2023). The Influence of the COVID-19 Pandemic on Social Anxiety: A Systematic Review. Int. J. Environ. Res. Public Health *20*, 2362. https://doi.org/10.3390/ijerph20032362.
8. Long, E., Patterson, S., Maxwell, K., Blake, C., Bosó Pérez, R., Lewis, R., McCann, M., Riddell, J., Skivington, K., Wilson-Lowe, R., and Mitchell, K.R. (2022). COVID-19 pandemic and its impact on social relationships and health. J. Epidemiol. Community. Health. *76*, 128–132. https://doi.org/10.1136/jech-2021-216690.
9. Forbes, P.A.G., Pronizius, E., Feneberg, A.C., Nater, U.M., Piperno, G., Silani, G., Stijovic, A., and Lamm, C. (2023). The effects of social interactions on momentary stress and mood during COVID-19 lockdowns. Br. J. Health Psychol. *28*, 306–319. https://doi.org/10.1111/bjhp.12626.
10. Ochsner, K.N., Silvers, J.A., and Buhle, J.T. (2012). Functional imaging studies of emotion regulation: a synthetic review and evolving model of the cognitive control of emotion. Ann. N. Y. Acad. Sci. *1251*, E1–E24.
11. Kim, S.H., and Hamann, S. (2007). Neural correlates of positive and negative emotion regulation. J. Cogn. Neurosci. *19*, 776–798. https://doi.org/10.1162/jocn.2007.19.5.776.
12. Wager, T.D., Davidson, M.L., Hughes, B.L., Lindquist, M.A., and Ochsner, K.N. (2008). Prefrontal-subcortical pathways mediating successful emotion regulation. Neuron *59*, 1037–1050. https://doi.org/10.1016/j.neuron.2008.09.006.
13. Keller, M., Mendoza-Quiñones, R., Cabrera Muñoz, A., Iglesias-Fuster, J., Virués, A.V., Zvyagintsev, M., Edgar, J.C., Zweerings, J., and Mathiak, K. (2022). Transdiagnostic alterations in neural emotion regulation circuits - neural substrates of cognitive reappraisal in patients with depression and post-traumatic stress disorder. BMC. Psychiatry. *22*, 173. https://doi.org/10.1186/s12888-022-03780-y.
14. Aron, A.R. (2007). The neural basis of inhibition in cognitive control. The Neuroscientist : a review journal bringing neurobiology. Neuroscientist *13*, 214–228. https://doi.org/10.1177/1073858407299288.
15. Tabibnia, G., Monterosso, J.R., Baicy, K., Aron, A.R., Poldrack, R.A., Chakrapani, S., Lee, B., and London, E.D. (2011). Different forms of self-control share a neurocognitive substrate. J. Neurosci. *31*, 4805–4810. https://doi.org/10.1523/JNEUROSCI.2859-10.2011.
16. Aron, A.R., Robbins, T.W., and Poldrack, R.A. (2004). Inhibition and the right inferior frontal cortex. Trends. Cogn. Sci. *8*, 170–177. https://doi.org/10.1016/j.tics.2004.02.010.
17. Light, S.N., Heller, A.S., Johnstone, T., Kolden, G.G., Peterson, M.J., Kalin, N.H., and Davidson, R.J. (2011). Reduced right ventrolateral prefrontal cortex activity while inhibiting positive affect is associated with improvement in hedonic capacity after 8 weeks of antidepressant treatment in major depressive disorder. Biol. Psychiatry. *70*, 962–968. https://doi.org/10.1016/j.biopsych.2011.06.031.
18. Yu, W., Li, Y., Cao, X., Mo, L., Chen, Y., and Zhang, D. (2023). The role of ventrolateral prefrontal cortex on voluntary emotion regulation of social pain. Hum. Brain Mapp. *44*, 4710–4721. https://doi.org/10.1002/hbm.26411.
19. Li, S., Xie, H., Zheng, Z., Chen, W., Xu, F., Hu, X., and Zhang, D. (2022). The causal role of the bilateral ventrolateral prefrontal cortices on emotion regulation of social feedback. Hum. Brain Mapp. *43*, 2898–2910. https://doi.org/10.1002/hbm.25824.
20. Reeck, C., Ames, D.R., and Ochsner, K.N. (2016). The Social Regulation of Emotion: An Integrative, Cross-Disciplinary Model. Trends Cogn. Sci. *20*, 47–63. https://doi.org/10.1016/j.tics.2015.09.003.
21. Koush, Y., Pichon, S., Eickhoff, S.B., Van De Ville, D., Vuilleumier, P., and Scharnowski, F. (2019). Brain networks for engaging oneself in positive-social emotion regulation. Neuroimage *189*, 106–115. https://doi.org/10.1016/j.neuroimage.2018.12.049.
22. Vrticka, P., Sander, D., and Vuilleumier, P. (2011). Effects of emotion regulation strategy on brain responses to the valence and social content of visual scenes. Neuropsychologia *49*, 1067–1082.
23. Vrticka, P., Sander, D., and Vuilleumier, P. (2012). Lateralized interactive social content and valence processing within the human amygdala. Frontiers *6*, 358. https://doi.org/10.3389/fnhum.2012.00358.
24. Banks, S.J., Eddy, K.T., Angstadt, M., Nathan, P.J., and Phan, K.L. (2007). Amygdala - frontal connectivity during emotion regulation. Soc. Cogn. Affect. Neurosci. *2*, 303–312. https://doi.org/10.1093/Scan/Nsm029.
25. Berboth, S., and Morawetz, C. (2021). Amygdala-prefrontal connectivity during emotion regulation: A meta-analysis of psychophysiological interactions. Neuropsychologia *153*, 107767. https://doi.org/10.1016/j.neuropsychologia.2021.107767.
26. Phelps, E.A., and LeDoux, J.E. (2005). Contributions of the amygdala to emotion processing: from animal models to human behavior. Neuron *48*, 175–187. https://doi.org/10.1016/j.neuron.2005.09.025.
27. Goossens, L., Kukolja, J., Onur, O.A., Fink, G.R., Maier, W., Griez, E., Schruers, K., and Hurlemann, R. (2009). Selective processing of social stimuli in the superficial amygdala. Hum. Brain. Mapp. *30*, 3332–3338. https://doi.org/10.1002/hbm.20755.
28. Fusar-Poli, P., Placentino, A., Carletti, F., Landi, P., Allen, P., Surguladze, S., Benedetti, F., Abbamonte, M., Gasparotti, R., Barale, F., et al. (2009). Functional atlas of emotional faces processing: a voxel-based meta-analysis of 105 functional magnetic resonance imaging studies. J. Psychiatry. Neurosci. *34*, 418–432.
29. Disner, S.G., Beevers, C.G., Haigh, E.A.P., and Beck, A.T. (2011). Neural mechanisms of the cognitive model of depression. Nat. Rev. Neurosci. *12*, 467–477. https://doi.org/10.1038/nrn3027.
30. Benschop, L., Vanhollebeke, G., Li, J., Leahy, R.M., Vanderhasselt, M.A., and Baeken, C. (2022). Reduced subgenual cingulate-dorsolateral

prefrontal connectivity as an electrophysiological marker for depression. Sci. Rep. *12*, 16903. https://doi.org/10.1038/s41598-022-20274-9.

31. Scharnowski, F., Nicholson, A.A., Pichon, S., Rosa, M.J., Rey, G., Eickhoff, S.B., Van De Ville, D., Vuilleumier, P., and Koush, Y. (2020). The role of the subgenual anterior cingulate cortex in dorsomedial prefrontal-amygdala neural circuitry during positive-social emotion regulation. Hum. Brain Mapp. *41*, 3100–3118. https://doi.org/10.1002/hbm.25001.
32. Premkumar, P. (2012). Are you being rejected or excluded? Insights from neuroimaging studies using different rejection paradigms. Clin. Psychopharmacol. Neurosci. *10*, 144–154. https://doi.org/10.9758/cpn.2012.10.3.144.
33. Lockwood, P.L., and Wittmann, M.K. (2018). Ventral anterior cingulate cortex and social decision-making. Neurosci. Biobehav. Rev. *92*, 187–191. https://doi.org/10.1016/j.neubiorev.2018.05.030.
34. Vetter, N.C., Weigelt, S., Döhnel, K., Smolka, M.N., and Kliegel, M. (2014). Ongoing neural development of affective theory of mind in adolescence. Soc. Cogn. Affect. Neurosci. *9*, 1022–1029. https://doi.org/10.1093/scan/nst081.
35. Klimecki, O.M. (2015). The plasticity of social emotions. Soc. Neurosci. *10*, 466–473. https://doi.org/10.1080/17470919.2015.1087427.
36. Roy, M., Shohamy, D., and Wager, T.D. (2012). Ventromedial prefrontal-subcortical systems and the generation of affective meaning. Trends Cogn. Sci. *16*, 147–156. https://doi.org/10.1016/j.tics.2012.01.005.
37. Braunstein, L.M., Gross, J.J., and Ochsner, K.N. (2017). Explicit and implicit emotion regulation: a multi-level framework. Soc. Cogn. Affect. Neurosci. *12*, 1545–1557. https://doi.org/10.1093/scan/nsx096.
38. Hiser, J., and Koenigs, M. (2018). The Multifaceted Role of the Ventromedial Prefrontal Cortex in Emotion, Decision Making, Social Cognition, and Psychopathology. Biol. Psychiatry *83*, 638–647. https://doi.org/10.1016/j.biopsych.2017.10.030.
39. Winecoff, A., Clithero, J.A., Carter, R.M., Bergman, S.R., Wang, L., and Huettel, S.A. (2013). Ventromedial prefrontal cortex encodes emotional value. J. Neurosci. *33*, 11032–11039. https://doi.org/10.1523/JNEUROSCI.4317-12.2013.
40. Sokolowski, A., Morawetz, C., Folkierska-Zukowska, M., and Lukasz Dragan, W. (2022). Brain activation during cognitive reappraisal depending on regulation goals and stimulus valence. Soc. Cognit. Affect Neurosci. *17*, 559–570. https://doi.org/10.1093/scan/nsab117.
41. Morawetz, C., Bode, S., Derntl, B., and Heekeren, H.R. (2017). The effect of strategies, goals and stimulus material on the neural mechanisms of emotion regulation: A meta-analysis of fMRI studies. Neurosci. Biobehav. Rev. *72*, 111–128. https://doi.org/10.1016/j.neubiorev.2016.11.014.
42. Li, F., Yin, S., Feng, P., Hu, N., Ding, C., and Chen, A. (2018). The cognitive up- and down-regulation of positive emotion: Evidence from behavior, electrophysiology, and neuroimaging. Biol. Psychol. *136*, 57–66. https://doi.org/10.1016/j.biopsycho.2018.05.013.
43. Morawetz, C., Riedel, M.C., Salo, T., Berboth, S., Eickhoff, S.B., Laird, A.R., and Kohn, N. (2020). Multiple large-scale neural networks underlying emotion regulation. Neurosci. Biobehav. Rev. *116*, 382–395. https://doi.org/10.1016/j.neubiorev.2020.07.001.
44. Dillon, D.G., and Pizzagalli, D.A. (2007). Inhibition of Action, Thought, and Emotion: A Selective Neurobiological Review. Appl. Prev. Psychol. *12*, 99–114. https://doi.org/10.1016/j.appsy.2007.09.004.
45. Aziz-Safaie, T., Müller, V.I., Langner, R., Eickhoff, S.B., and Cieslik, E.C. (2024). The effect of task complexity on the neural network for response inhibition: An ALE meta-analysis. Neurosci. Biobehav. Rev. *158*, 105544. https://doi.org/10.1016/j.neubiorev.2024.105544.
46. Zeidman, P., Jafarian, A., Corbin, N., Seghier, M.L., Razi, A., Price, C.J., and Friston, K.J. (2019). A guide to group effective connectivity analysis, part 1: First level analysis with DCM for fMRI. Neuroimage *200*, 174–190.
47. Zeidman, P., Jafarian, A., Seghier, M.L., Litvak, V., Cagnan, H., Price, C.J., and Friston, K.J. (2019). A guide to group effective connectivity analysis, part 2: Second level analysis with PEB. Neuroimage *200*, 12–25.
48. Snippe, E., Jeronimus, B.F., Aan Het Rot, M., Bos, E.H., de Jonge, P., and Wichers, M. (2018). The Reciprocity of Prosocial Behavior and Positive Affect in Daily Life. J. Pers. *86*, 139–146. https://doi.org/10.1111/jopy.12299.
49. Aknin, L.B., Van de Vondervoort, J.W., and Hamlin, J.K. (2018). Positive feelings reward and promote prosocial behavior. Curr. Opin. Psychol. *20*, 55–59. https://doi.org/10.1016/j.copsyc.2017.08.017.
50. Alexander, R., Aragón, O.R., Bookwala, J., Cherbuin, N., Gatt, J.M., Kahrilas, I.J., Kästner, N., Lawrence, A., Lowe, L., Morrison, R.G., et al. (2021). The neuroscience of positive emotions and affect: Implications for cultivating happiness and wellbeing. Neurosci. Biobehav. Rev. *121*, 220–249. https://doi.org/10.1016/j.neubiorev.2020.12.002.
51. Vrticka, P., Bondolfi, G., Sander, D., and Vuilleumier, P. (2012). The neural substrates of social emotion perception and regulation are modulated by adult attachment style. Soc. Neurosci. *7*, 473–493. https://doi.org/10.1080/17470919.2011.647410.
52. Bickart, K.C., Dickerson, B.C., and Barrett, L.F. (2014). The amygdala as a hub in brain networks that support social life. Neuropsychologia *63*, 235–248. https://doi.org/10.1016/j.neuropsychologia.2014.08.013.
53. Goldberg, I.I., Harel, M., and Malach, R. (2006). When the brain loses its self: prefrontal inactivation during sensorimotor processing. Neuron *50*, 329–339. https://doi.org/10.1016/j.neuron.2006.03.015.
54. Ochsner, K.N., and Gross, J.J. (2008). Cognitive emotion regulation: Insights from social cognitive and affective neuroscience. Curr. Dir. Psychol. Sci. *17*, 153–158. https://doi.org/10.1111/j.1467-8721.2008.00566.x.
55. Amodio, D.M., and Frith, C.D. (2006). Meeting of minds: the medial frontal cortex and social cognition. Nat. Rev. Neurosci. *7*, 268–277. https://doi.org/10.1038/nrn1884.
56. Bzdok, D., Langner, R., Schilbach, L., Engemann, D.A., Laird, A.R., Fox, P.T., and Eickhoff, S.B. (2013). Segregation of the human medial prefrontal cortex in social cognition. Front. Hum. Neurosci. *7*, 232. https://doi.org/10.3389/fnhum.2013.00232.
57. Gusnard, D.A., Akbudak, E., Shulman, G.L., and Raichle, M.E. (2001). Medial prefrontal cortex and self-referential mental activity: relation to a default mode of brain function. Proc. Natl. Acad. Sci. USA *98*, 4259–4264. https://doi.org/10.1073/pnas.071043098.
58. Drabant, E.M., McRae, K., Manuck, S.B., Hariri, A.R., and Gross, J.J. (2009). Individual differences in typical reappraisal use predict amygdala and prefrontal responses. Biol. Psychiatry *65*, 367–373. https://doi.org/10.1016/j.biopsych.2008.09.007.
59. Gao, W., Biswal, B., Chen, S., Wu, X., and Yuan, J. (2021). Functional coupling of the orbitofrontal cortex and the basolateral amygdala mediates the association between spontaneous reappraisal and emotional response. Neuroimage *232*, 117918. https://doi.org/10.1016/j.neuroimage.2021.117918.
60. Kanske, P., Heissler, J., Schönfelder, S., and Wessa, M. (2012). Neural correlates of emotion regulation deficits in remitted depression: the influence of regulation strategy, habitual regulation use, and emotional valence. Neuroimage *61*, 686–693. https://doi.org/10.1016/j.neuroimage.2012.03.089.
61. Fitzgerald, J.M., MacNamara, A., Kennedy, A.E., Rabinak, C.A., Rauch, S.A.M., Liberzon, I., and Phan, K.L. (2017). Individual differences in cognitive reappraisal use and emotion regulatory brain function in combat-exposed veterans with and without PTSD. Depress. Anxiety. *34*, 79–88. https://doi.org/10.1002/da.22551.
62. Morawetz, C., Bode, S., Baudewig, J., and Heekeren, H.R. (2017). Effective amygdala-prefrontal connectivity predicts individual differences in successful emotion regulation. Soc. Cogn. Affect. Neurosci. *12*, 569–585. https://doi.org/10.1093/scan/nsw169.
63. He, Z., Li, S., Mo, L., Zheng, Z., Li, Y., Li, H., and Zhang, D. (2023). The VLPFC-Engaged Voluntary Emotion Regulation: Combined TMS-fMRI Evidence for the Neural Circuit of Cognitive Reappraisal. J. Neurosci. *43*, 6046–6060. https://doi.org/10.1523/JNEUROSCI.1337-22.2023.

64. Steward, T., Davey, C.G., Jamieson, A.J., Stephanou, K., Soriano-Mas, C., Felmingham, K.L., and Harrison, B.J. (2021). Dynamic Neural Interactions Supporting the Cognitive Reappraisal of Emotion. Cereb. Cortex. *31*, 961–973. https://doi.org/10.1093/cercor/bhaa268.

65. Britton, J.C., Phan, K.L., Taylor, S.F., Welsh, R.C., Berridge, K.C., and Liberzon, I. (2006). Neural correlates of social and nonsocial emotions: An fMRI study. Neuroimage *31*, 397–409. https://doi.org/10.1016/j.neuroimage.2005.11.027.

66. Hare, T.A., Camerer, C.F., Knoepfle, D.T., and Rangel, A. (2010). Value computations in ventral medial prefrontal cortex during charitable decision making incorporate input from regions involved in social cognition. J. Neurosci. *30*, 583–590. https://doi.org/10.1523/JNEUROSCI.4089-09.2010.

67. Adolphs, R., Baron-Cohen, S., and Tranel, D. (2002). Impaired recognition of social emotions following amygdala damage. J. Cogn. Neurosci. *14*, 1264–1274. https://doi.org/10.1162/089892902760807258.

68. Padilla-Coreano, N., Tye, K.M., and Zelikowsky, M. (2022). Dynamic influences on the neural encoding of social valence. Nat. Rev. Neurosci. *23*, 535–550. https://doi.org/10.1038/s41583-022-00609-1.

69. McRae, K., Ochsner, K.N., Mauss, I.B., Gabrieli, J.J.D., and Gross, J.J. (2008). Gender Differences in Emotion Regulation: An fMRI Study of Cognitive Reappraisal. Group Process. Intergroup Relat. *11*, 143–162. https://doi.org/10.1177/1368430207088035.

70. Gaviria, J., Rey, G., Bolton, T., Ville, D.V.D., and Vuilleumier, P. (2021). Dynamic functional brain networks underlying the temporal inertia of negative emotions. Neuroimage *240*, 118377. https://doi.org/10.1016/j.neuroimage.2021.118377.

71. Koush, Y., Meskaldji, D.E., Pichon, S., Rey, G., Rieger, S.W., Linden, D.E.J., Van De Ville, D., Vuilleumier, P., and Scharnowski, F. (2017). Learning Control Over Emotion Networks Through Connectivity-Based Neurofeedback. Cereb. Cortex *27*, 1193–1202. https://doi.org/10.1093/cercor/bhv311.

72. Young, K.D., Siegle, G.J., Zotev, V., Phillips, R., Misaki, M., Yuan, H., Drevets, W.C., and Bodurka, J. (2017). Randomized Clinical Trial of Real-Time fMRI Amygdala Neurofeedback for Major Depressive Disorder: Effects on Symptoms and Autobiographical Memory Recall. Am. J. Psychiatry. *174*, 748–755. https://doi.org/10.1176/appi.ajp.2017.16060637.

73. Grosse Rueschkamp, J.M., Brose, A., Villringer, A., and Gaebler, M. (2019). Neural correlates of up-regulating positive emotions in fMRI and their link to affect in daily life. Soc. Cogn. Affect. Neurosci. *14*, 1049–1059. https://doi.org/10.1093/scan/nsz079.

74. Lang, P.J., Greenwald, M.K., Bradley, M.M., and Hamm, A.O. (1993). Looking at pictures: affective, facial, visceral, and behavioral reactions. Psychophysiology *30*, 261–273. https://doi.org/10.1111/j.1469-8986.1993.tb03352.x.

75. Marchewka, A., Zurawski, Ł., Jednoróg, K., and Grabowska, A. (2014). The Nencki Affective Picture System (NAPS): introduction to a novel, standardized, wide-range, high-quality, realistic picture database. Behav. Res. Methods *46*, 596–610. https://doi.org/10.3758/s13428-013-0379-1.

76. Kurdi, B., Lozano, S., and Banaji, M.R. (2017). Introducing the Open Affective Standardized Image Set (OASIS). Behav. Res. Methods *49*, 457–470. https://doi.org/10.3758/s13428-016-0715-3.

77. Weierich, M.R., Kleshchova, O., Rieder, J.K., and Reilly, D.M. (2019). The Complex Affective Scene Set (COMPASS): Solving the Social Content Problem. Affective Visual Stimulus Sets *5*, 53. https://doi.org/10.1525/collabra.256.

78. Crone, D.L., Bode, S., Murawski, C., and Laham, S.M. (2018). The Socio-Moral Image Database (SMID): A novel stimulus set for the study of social, moral and affective processes. PLoS One *13*, e0190954. https://doi.org/10.1371/journal.pone.0190954.

79. Dan-Glauser, E.S., and Scherer, K.R. (2011). The Geneva affective picture database (GAPED): a new 730-picture database focusing on valence and normative significance. Behav. Res. Methods *43*, 468–477. https://doi.org/10.3758/s13428-011-0064-1.

80. Carretié, L., Tapia, M., López-Martín, S., and Albert, J. (2019). EmoMadrid: An emotional pictures database for affect research. Motiv. Emot. *43*, 929–939. https://doi.org/10.1007/s11031-019-09780-y.

81. Bradley, M.M., and Lang, P.J. (1994). Measuring emotion: the Self-Assessment Manikin and the Semantic Differential. J. Behav. Ther. Exp. Psychiatry. *25*, 49–59. https://doi.org/10.1016/0005-7916(94)90063-9.

82. Gross, J.J., and John, O.P. (2003). Individual differences in two emotion regulation processes: implications for affect, relationships, and well-being. J. Pers. Soc. Psychol. *85*, 348–362. https://doi.org/10.1037/0022-3514.85.2.348.

83. Beck, A.T., Steer, R.A., Ball, R., and Ranieri, W. (1996). Comparison of Beck Depression Inventories -IA and -II in psychiatric outpatients. J. Pers. Assess. *67*, 588–597. https://doi.org/10.1207/s15327752jpa6703_13.

84. Zigmond, A.S., and Snaith, R.P. (1983). The hospital anxiety and depression scale. Acta. Psychiatr. Scand. *67*, 361–370. https://doi.org/10.1111/j.1600-0447.1983.tb09716.x.

85. Spielberger, C., Gorsuch, R., Lushene, R., Vagg, P.R., and Jacobs, G. (1983). Manual for the State-Trait Anxiety Inventory (Form Y1 – Y2);Consulting Psychologists (Palo Alto, CA, USA: Press).

86. Mishlove, M., and Chapman, L.J. (1985). Social anhedonia in the prediction of psychosis proneness. J. Abnorm. Psychol. *94*, 384–396. https://doi.org/10.1037//0021-843x.94.3.384.

87. Snaith, R.P., Hamilton, M., Morley, S., Humayan, A., Hargreaves, D., and Trigwell, P. (1995). A scale for the assessment of hedonic tone the Snaith-Hamilton Pleasure Scale. Br. J. Psychiatry. *167*, 99–103. https://doi.org/10.1192/bjp.167.1.99.

88. Treynor, W., Gonzalez, R., and Nolen-Hoeksema, S. (2003). Rumination Reconsidered: A Psychometric Analysis. Cognit. Ther. Res. *27*, 247–259. https://doi.org/10.1023/A:1023910315561.

89. Brennan, K.A., Clark, C.L., and Shaver, P. (1998). Self-report measurement of adult attachment: An integrative overview. In Attachment theory and close relationships, J. A. Simpson and W. S. Rholes, eds. (The Guilford Press), pp. 46–76.

90. Carver, C.S., and White, T.L. (1994). Behavioral inhibition, behavioral activation, and affective responses to impending reward and punishment: The BIS/BAS Scales. J. Pers. Soc. Psychol. *67*, 319–333. https://doi.org/10.1037/0022-3514.67.2.319.

91. Rotter, J.B. (1966). Generalized expectancies for internal versus external control of reinforcement. Psychol. Monogr. *80*, 1–28. https://doi.org/10.1037/h0092976.

92. Watson, D., Clark, L.A., and Tellegen, A. (1988). Development and validation of brief measures of positive and negative affect: the PANAS scales. J. Pers. Soc. Psychol. *54*, 1063–1070. https://doi.org/10.1037//0022-3514.54.6.1063.

93. Jenkinson, M. (2003). Fast, automated, N-dimensional phase-unwrapping algorithm. Magn. Reson. Med. *49*, 193–197. https://doi.org/10.1002/mrm.10354.

94. Ashburner, J. (2007). A fast diffeomorphic image registration algorithm. Neuroimage *38*, 95–113. https://doi.org/10.1016/j.neuroimage.2007.07.007.

95. Power, J.D., Barnes, K.A., Snyder, A.Z., Schlaggar, B.L., and Petersen, S.E. (2012). Spurious but systematic correlations in functional connectivity MRI networks arise from subject motion. Neuroimage *59*, 2142–2154. https://doi.org/10.1016/j.neuroimage.2011.10.018.

96. Krylova, M., Skouras, S., Razi, A., Nicholson, A.A., Karner, A., Steyrl, D., Boukrina, O., Rees, G., Scharnowski, F., and Koush, Y. (2021). Progressive modulation of resting-state brain activity during neurofeedback of positive-social emotion regulation networks. Sci. Rep. *11*, 23363. https://doi.org/10.1038/s41598-021-02079-4.

97. Rolls, E.T., Huang, C.C., Lin, C.P., Feng, J., and Joliot, M. (2020). Automated anatomical labelling atlas 3. Neuroimage *206*, 116189. https://doi.org/10.1016/j.neuroimage.2019.116189.

98. Palomero-Gallagher, N., Eickhoff, S.B., Hoffstaedter, F., Schleicher, A., Mohlberg, H., Vogt, B.A., Amunts, K., and Zilles, K. (2015). Functional organization of human subgenual cortical areas: Relationship between architectonical segregation and connectional heterogeneity. Neuroimage *115*, 177–190. https://doi.org/10.1016/j.neuroimage.2015.04.053.

99. Friston, K.J., Harrison, L., and Penny, W. (2003). Dynamic causal modelling. Neuroimage *19*, 1273–1302.

100. Friston, K., Mattout, J., Trujillo-Barreto, N., Ashburner, J., and Penny, W. (2007). Variational free energy and the Laplace approximation. Neuroimage *34*, 220–234. https://doi.org/10.1016/j.neuroimage.2006.08.035.

101. Guedj, C., and Vuilleumier, P. (2023). Modulation of pulvinar connectivity with cortical areas in the control of selective visual attention. Neuroimage *266*, 119832. https://doi.org/10.1016/j.neuroimage.2022.119832.

STAR★METHODS

KEY RESOURCES TABLE

REAGENT or RESOURCE	SOURCE	IDENTIFIER
Deposited data		
Group level fMRI contrasts	OSF repository	https://osf.io/8tvec/
Single subject DCM	OSF repository	https://osf.io/8tvec/
Individual ROI masks	OSF repository	https://osf.io/8tvec/
Single subject raw data	Federal Research Center of Fundamental and Translational Medicine	N/A
Software and algorithms		
MATLAB R2021b	MathWorks, Natick, MA	https://www.mathworks.com/products/matlab.html
Statistical Parametric Mapping (SPM12, v7771), including DCM 12.5	Wellcome Trust Center for Neuroimaging	https://www.fil.ion.ucl.ac.uk/spm/

EXPERIMENTAL MODEL AND STUDY PARTICIPANT DETAILS

Participants

We used previously published fMRI data[21] from twenty-three healthy participants (11 female, mean ± SD age, 27.7 ± 6.2 years, White cohort), denoted as the first experiment, and newly collected data of twenty-one healthy females aged between 18 and 55 who were recruited for a single day study, denoted as the second experiment. One subject was excluded from new data due to excessive head movements in fMRI session, leaving a sample of 20 participants (mean ± SD age, 37.1 ± 8.4 years, White cohort). For the second experiment, we recruited only female participants, because prior work suggests they show stronger emotional responses and larger regulation effects in both PFC and subcortical areas, as compared to males, particularly for positive emotions and reappraisal.[69,70] They reported no history of neurological, psychiatric, or addictive disorders as well as no contraindications to MR imaging, were free of any psychotropic medication, and had normal or corrected-to-normal vision.

Informed consent and ethics approval

The first experiment was approved by the ethics committee at the University of Geneva, Geneva, Switzerland.[21] The second experiment was approved by the ethics review board of the Federal research center of fundamental and translational medicine, Novosibirsk, Russian Federation (approval number 28/1). All participants gave written informed consent prior to the study and received a monetary compensation.

METHOD DETAILS

Stimuli

For both experiments, a set of social pictures was collected from the International Affective Pictures System (IAPS),[74] Nencki Affective Picture System (NAPS),[75] Open Affective Standardized Image Set (OASIS),[76] Complex Affective Scene Set (COMPASS),[77] Socio-Moral Image Database (SMID),[78] Geneva Affective Picture Database (GAPED),[79] and EMOMadrid database[80] (901 in total). Pictures were classified as social based on presence of people and faces as a part of the scene.[65] Pictures were resized to fit the screen resolution of display monitor; no additional cropping and color correction was performed. To account for relative biases in valence and arousal scores between different image databases, we matched their scores given predefined categories with uniform emotional response, e.g., weddings, happy babies, team sports, smiling adults, etc. Using linear regression model, we examined the association between median valence and arousal scores of each category and recoded original scores to those in IAPS. We did not include extreme positive content to avoid ceiling effects. The order of image presentation for fMRI scans and behavioral ratings was pseudo-randomized per participant. For average values, we reported the mean and standard deviation (SD).

For the first experiment, stimuli details are listed elsewhere (positive social pictures, $n = 112$, normative valence 6.97 ± 0.68, arousal 4.97 ± 0.82; neutral nonsocial pictures, $n = 112$, normative valence 5.21 ± 0.60, arousal 3.61 ± 0.96).[21] For the second experiment, stimuli were assigned to positive social pictures ($n = 369$, normative valence 7.13 ± 0.34, arousal 4.97 ± 0.65) or neutral social pictures ($n = 420$, normative valence 5.32 ± 0.78, arousal 4.35 ± 0.48). Social pictures were used for fMRI sessions and behavioral ratings of valence, arousal, and sociality after fMRI. Pictures used for fMRI and behavioral sets did not overlap.

Stimuli selected for the fMRI set in the second experiment comprised a series of different pseudo-randomized 120 positive social (group average; normative valence = 7.11 ± 0.01, arousal = 4.94 ± 0.03) and 150 neutral social pictures (group average; normative valence = 5.35 ± 0.01, arousal = 4.28 ± 0.03). Positive and neutral social pictures were significantly different on the subject level (two-sample one-tailed t-test, p-values <0.001), which was also confirmed on the trial level (two-sample one-tailed t-test; valence p-values <0.001; arousal p-values <0.015). For positive and neutral social between-subject stimuli randomizations, we minimized the difference in valence (two-sample two-tailed t-test; positive p-values >0.76, neutral p-values >0.72) and arousal (two-sample two-tailed t-test; positive p-values >0.50, neutral p-values >0.23).

Stimuli selected for the behavioral rating sets (30 pictures each; group average; positive social normative valence = 7.15 ± 0.03, arousal = 5.06 ± 0.04, neutral social normative valence = 5.27 ± 0.03, arousal = 4.46 ± 0.04) were also pseudo-randomized and had significant difference in valence between sets (two-sample one-tailed t-test; p-values <0.001) and in arousal between neutral and positive pictures (two-sample one-tailed t-test, p-values <0.002). For both categories, we minimized between-subject difference in valence (two-sample two-tailed t-test; positive social p-values >0.38; neutral social p-values >0.66) and arousal (two-sample t-test; positive social p-values >0.62; neutral social p-values >0.50). Social pictures from behavioral and fMRI picture sets did not differ in valence (two-sample t-test; positive p-values >0.37; neutral p-values >0.34) and arousal (two-sample t-test; positive p-values >0.13; neutral p-values >0.13).

Each picture was repeated a limited number of times per group (median [quartiles] = 6 [3 10]). For individual picture sets, the mean normative valence and arousal was significantly greater for positive than neutral social pictures (two-sample one-tailed t-test; valence p-values <0.001, arousal p-values <0.002). There was no significant difference in valence and arousal between fMRI and behavioral picture sets (p-values >0.13).

Experimental paradigm

The first experiment was set as a 2 × 2 factorial design based on the factors stimuli (positive-social vs. neutral nonsocial scenes) and task (passive viewing vs. effortful emotion upregulation).[21] For design efficiency and stronger signal to noise, we did not manipulate valence and content of pictures separately,[22,65] because this study did not aim at dissecting these two factors but focused on positive aspects of social interactions only.[21] We acquired two functional runs (11.3 min run duration) consisting of two emotion upregulation or passive viewing epochs randomized across subjects (alternating seven blocks of positive social and neutral nonsocial pictures per epoch, 4 pictures per block, 6s picture display duration).

Because the first experiment allows contrasting upregulation and passive viewing of positive social pictures, in the second experiment we included only the critical experimental condition with upregulation of positive social pictures, and a reference baseline condition with passive viewing of neutral social pictures,[12] allowing our analysis to most effectively capture upregulation effects for social stimuli.[73] Our experimental design is particularly different from previous factorial studies[22,40] by balanced passive viewing of neutral social scenes and fixation baseline. We contrasted blocks of positive social upregulation and neutral social viewing in two subsequent fMRI runs (Figure 1; 17.6min run duration). Both runs consisted of five trials alternating four emotion regulation blocks with five passive viewing (3 pictures per block with 18s display duration) plus a fixation cross presented for 48s. For both experiments during positive social upregulation blocks, subjects were asked to imagine active and enjoyable interactions with people depicted in social pictures from a first-person perspective. During neutral social viewing blocks, subjects were asked to passively look at neutral social pictures. Stimuli and tasks were indicated by different picture frame colors. The stimuli were presented on the screen of an MR-compatible monitor visible through a mirror attached to the head coil. All participants were instructed to breathe steadily and remain as still as possible.

After fMRI runs of the second experiment, participants performed a behavioral rating task with two picture sets (60 pictures in total), using valence and arousal scores on a continuous scale of self-assessment manikins.[81] For sociality ratings, they evaluated how much socially engaging or interacting they felt about depicted scenes using customized manikins representing incremental increases in sociality. Care was taken to ensure that participants did not make their rating depending on the number of people in the scene, for example if there is only one person, they could base their rating on how easily they could interact with that person in this scene. Understanding of the task was ensured and response time was not limited.

To assess personality traits that may influence changes in brain activity and connectivity, participants were asked to complete the Emotion Regulation Questionnaire (ERQ),[82] Beck Depression Inventory-II (BDI),[83] Hospital Anxiety and Depression Scale (HADS),[84] State-Trait Anxiety Inventory (STAI),[85] Revised Social Anhedonia Scale (RSAS),[86] Snaith-Hamilton Pleasure Scale (SHAPS),[87] Ruminative Response Scale (RRS),[88] Experiences in Close Relationships questionnaire (ECR),[89] Behavioral Inhibition and Activation Systems Scales (BIS/BAS),[90] and Rotter's Internal-External Locus of Control Scale (LCS).[91]

To test whether emotional state changes after upregulation fMRI session, we measured the Positive and Negative Affect Schedule (PANAS)[92] before and after this session. To assess compliance with instructions and strategy details, we asked participants to rate whether they were focused or absentminded, and whether their imagery was vivid or not (Likert scale from −5 to +5).

MRI data acquisition

The first experiment was performed on a 3T MRI scanner (Trio Tim, Siemens Medical Solutions, Erlangen, Germany) equipped with a 32-channel head coil at the Brain and Behavior Laboratory (University of Geneva). Functional images were acquired with a whole-brain single-shot gradient-echo T2*-weighted EPI sequence (TR/TE = 2050/35ms, flip angle = 75°, matrix 120 × 120, 32 slices, voxel size 2 × 2 × 2mm^3, GRAPPA, iPAT = 3).

For the second experiment, MRI recordings were performed on a 3T MRI scanner (Ingenia, Philips, Best, the Netherlands) equipped with a 16-channel head coil at the International Tomography Center SB RAS. A T1-weighted structural image was acquired at the beginning of the scanning session using 3D turbo field echo sequence with TR/TE = 7.7/3.8ms, flip angle = 8°, matrix 288 × 288, 181 slices, and voxel size = 0.87 × 0.87 × 1mm^3. Functional T2*-weighted images (528 scans per run) were obtained with a single-shot gradient-echo EPI sequence with TR/TE = 2000/35ms, flip angle = 90°, matrix 112 × 112, 31 slices, voxel size 2 × 2 × 3mm^3, 9 dummy scans, and parallel imaging (SENSE) factor = 3. The EPI protocol was configured to maximize brain coverage and to ensure optimal signal quality for sgACC and bilateral amygdala.[31] We also acquired a double-echo gradient-echo static magnetic field map (TE_1 = 7ms, TE_2 = 10ms, flip angle = 70°, voxel size = 2.5 × 2.5 × 2.5mm^3).

fMRI data preprocessing

For both experiments, the conventional fMRI data processing was performed using SPM12 (Wellcome Trust Center for Neuroimaging, Queen Square, London, UK) and MATLAB (Mathworks, Inc.). The functional images were spatially realigned to the first scan of each run, corrected for slice-timing and geometric distortions,[93] co-registered to the individual structural image, normalized to the standard MNI structural template with an isotropic 2mm^3 voxel size and smoothed with an isotropic Gaussian kernel with 6mm full-width-at-half-maximum (FWHM) using DARTEL.[94]

QUANTIFICATION AND STATISTICAL ANALYSIS

GLM analysis

First-level fMRI analysis for the first experiment is described in detail elsewhere.[21] Similarly for the second experiment at the single-subject level, we specified a general linear model (GLM) with a separate regressor for each trial of passive viewing and emotion upregulation conditions, implemented in SPM12. For two functional runs the fixed-effect model was applied. We modeled regressors as boxcar functions convolved with the canonical hemodynamic response function (HRF), 6 head movement covariates to capture residual motion artifacts, and removed scans with excessive head motion (framewise displacement >0.9).[95,96] The data were high-pass filtered with a conventional 0.008Hz cut-off.

For the second experiment whole-brain group-level analysis, a flexible factorial ANOVA was performed with a random factor 'subject' and fixed factor 'condition' (trial-based individual contrasts). As contrasts of interest, we computed upregulate positive vs. view neutral and upregulate positive vs. fixation. Statistical maps were corrected for multiple comparisons using whole brain family-wise error correction (FWE, $p < 0.05$).

Dynamic causal modeling

Definition of individual regions of interest

For DCM estimations, we defined group and individual ROIs. Group ROIs were defined within corresponding anatomical structures and served as reference areas within which individual functional peaks of activity were located.[46] Group ROIs did not overlap. Group bilateral amygdala ROIs were defined anatomically based on the AAL3 atlas[97] because it is a small region for which a spherical ROI would have likely included non-amygdala voxels in proximity. Group sgACC ROI was defined as an anatomically referenced 16 × 27 × 12mm^3 box centered at [0,14,-12] with the addition of a Brodman Area 25.[98] To localize other key network nodes, we used 8mm spheres centered on ROI peak coordinates at the group level (FWE, $p < 0.05$). Group vmPFC ([-2, 56, −18]), SFG (left, [-16, 54, 38]; right, [16, 50, 44]; central dmPFC: [-2, 58, 36]), and pvlPFC (left, [-56, 24, 12]; right, [58, 28, 4]) maxima were defined using upregulate positive > view neutral contrast. For group arvlPFC, we used peak coordinates [46, 41, −4] defined as the intersection between view neutral > upregulate positive contrast and bilateral vlPFC maps extracted from Neurosynth database (association tests, entry "inhibitory control" and "ventrolateral prefrontal"). The group arvlPFC ROI is in good agreement with emotion regulation studies[12] and in relatively close proximity yet different from more posterior inferior frontal gyrus areas involved in reappraisal of positive and negative emotions[40,43] and inhibitory control.[44,45]

For DCM node time-series extraction, individual ROIs were defined as spheres of 6mm radius centered on the peaks located within corresponding group ROIs using individual contrast maps exceeded a liberal statistical threshold ($p < 0.05$ unc.). Individual sgACC ROI was defined as a small rectangle around individual peak using upregulate positive > fixation contrast. In case of absence of individual maximum, we used a group ROI mask. Individual sgACC and bilateral amygdala ROIs were restricted by corresponding group masks.

PEB DCM analysis

For the second experiment, to model functional networks engaged during the task, we applied bilinear Dynamic Causal Modeling (DCM). DCM is a Bayesian framework that evaluates directional interactions between different brain areas (i.e., effective connectivity) and the impact of experimental tasks on these interactions. DCM combines biologically plausible neurovascular model with neuronal model to predict observed fMRI time-series and estimate model parameters using Variational Bayes under a fixed-form Laplace scheme.[99,100] Functional brain network was modeled as endogenous bidirectional connectivity between the DCM model nodes and self-connectivity of nodes (matrix A), plus modulatory inputs onto the endogenous connections related to contextual factors (i.e., engaging actively in the depicted situations, matrix B) and external inputs (i.e., presentation of stimuli, matrix C). Non-diagonal elements of matrices A and B indicate the rate of change in response of one region that is caused by activity in another region without

external perturbations or modulated by contextual factors, respectively (in Hz). Positive connectivity strength describes excitatory influences, while negative value represents inhibitory influences. The diagonal elements refer to self-inhibition processes.

To infer the effective connectivity parameters at the first and second level analyses, we used the Parametric Empirical Bayes (PEB) framework as implemented in SPM12.[47] This hierarchical approach allows estimations of the fully connected DCM models using network node time-series and evaluations of the nested (reduced) network models using Bayesian model reduction (BMR).

At the first level, we estimated individual fully connected bilinear DCM models of six key nodes. Based on previous research[12,21,22,31,40] and current findings, six ROIs centered around the individual functional activity peaks referenced to the correspondent anatomical structures and group ROIs were considered as key nodes of emotion regulation and social behavior network. These nodes included arvlPFC, bilateral posterior ventrolateral prefrontal cortex (pvlPFC), bilateral amygdala (AMY), dmPFC along with adjacent bilateral superior frontal gyrus (SFG), sgACC, and vmPFC. For each individual ROI average time-series, we regressed out head motion parameters, linear trend, and constant term using GLM, and high-pass filtered with 0.008Hz cutoff. We averaged bilateral SFG, pvlPFC and AMY time-series across left and right hemispheres.[21,101] For fully connected DCM models, the external stimuli influenced all six model nodes (i.e., picture presentation conditions), as well as contextual modulations (i.e., emotion regulation condition) influenced bidirectional connections and not self-inhibitory.

At the second level, we identified the PEB network models and their parameters that describe group average endogenous connections and their contextual modulations for emotion regulation processes, as well as network architectures associated with individual sociality scores applied as covariates. In the PEB framework, this was accomplished by comparing the evidence of the reduced models with certain combinations of parameters switched off, which could be derived analytically from the full model using Bayesian Model Reduction (BMR).[47] Specifically, network models varied separately for endogenous connections between nodes (i.e., comparing evidence for reduced endogenous connectivity models, matrix A) and contextual modulations of functional coupling strengths between nodes (i.e., comparing evidence for reduced contextual connectivity models, matrix B). We used an automatic model search over all possible reduced network models to identify parameters that did not contribute to the model evidence. Bayesian Model Averaging (BMA) over 256 best models from the last iteration of the model search procedure was used to reveal the most plausible endogenous connections and contextual modulations, respectively. The posterior probability (Pp) for each PEB parameter was calculated by comparing the evidence of all models which had the corresponding connectivity parameter switched on, versus all models which had that parameter switched off. The $Pp > 0.95$ corresponds to the strong evidence.

Analyses of the behavioral and psychometric data

For the second experiment, we performed a cross-correlation analysis of behavioral ratings and psychometric scores using Pearson correlation. We also investigated associations between individual brain activity, connectivity, psychometric scores, and behavioral ratings with focus on sociality scores of neutral and positive social pictures. For ROI activity estimates, we extracted whole-brain GLM contrast betas (“upregulate positive social - view neutral social pictures”, “upregulate positive social - fixation”). For ROI connectivity estimates, we performed the follow-up correlations for illustration purposes. The statistical significance was corrected for multiple comparisons using false discovery rate (FDR, $p < 0.05$). For average values, we reported the mean and standard deviation (SD).